2008 IEEE International Conference on
Robotics and Automation
Pasadena, CA, USA, May 19-23, 2008

Direct Kinematics of Zero-Torsion Parallel Mechanisms

Ilian A. Bonev
Department of Automated Manufacturing Engineering
École de technologie supérieure
1100 Notre-Dame St. W., Montreal, QC, Canada H3C 1K3
ilian.bonev@etsmtl.ca

***Abstract*— This paper presents the closed-form solutions to the direct kinematics of three 3-DOF symmetric zero-torsion parallel mechanisms. These mechanisms are composed of three identical legs ending with a spherical joint that is constrained to move in one of three equally spaced planes intersecting at one line. The closed-form solutions are based on the use of a not-well-known intuitive orientation representation. The latter, previously introduced under the name of Tilt-and-Torsion angles, is briefly described. Then, the interdependence between the Cartesian coordinates of the general class of parallel mechanisms is derived. Finally, the direct kinematics of the mechanisms are derived and numerical examples are presented.**

I. INTRODUCTION

Since the late 1990s, when it became clear that hexapods are too complex for machining applications, industry and academia have spent considerable efforts on investigating parallel mechanisms with less than six degrees of freedom (DOF) [1]. The most popular of these are undoubtedly the group of 3-DOF parallel mechanisms whose mobile platform is attached to three legs via spherical joints (Fig. 1) and has two rotational and one translational DOFs. The legs constrain the centers of the spherical joints to move in three equally spaced vertical planes intersecting at a common line. These mechanisms will be referred to as 3-*[PP]S* ones.[1]

There is abundant literature on this group of mechanisms. To name a few examples, a 3-$\underline{P}PS$ parallel mechanism was proposed in [2] (Fig. 1a), the 3-$R\underline{P}S$ architecture (Fig. 1b) was analyzed in [3]-[7], two different 3-$\underline{P}RS$ designs were studied in [8] (Fig. 1c) and [9] (Fig. 1d), the latter design being best known through the patented *Z3 Head* by DS Technologie [10], and finally a 3-$\underline{R}RS$ manipulator was investigated in [11]. Of all these publications, only [4] seems to identify the exact nature of the interdependence of the orientation parameters and its geometric significance. To fill this important gap, we studied the kinematic geometry of 3-*[PP]S* parallel mechanisms as well as of two other groups of mechanisms and showed clearly their motion pattern [12].

While the direct kinematics of any parallel mechanism can be solved by an iterative numerical method, a closed-form solution is clearly preferred. Such a solution is not only more accurate but gives a valuable insight for the design stage. Perhaps due to the lack of clear understanding of the kinematic geometry of 3-*[PP]S* parallel mechanisms, no analytic procedure for their direct kinematics has ever been proposed in literature. The only exception could be [6], where the authors propose an approach for solving the direct kinematics of the 3-$\underline{P}RS$ parallel mechanism of Fig. 1(d), but they obtain a total of 64 solutions, yet there are only 16 [13].

In this paper, we use a special orientation representation to obtain closed-form solutions to the direct kinematics of several 3-*[PP]S* parallel mechanisms. In the next section, we describe briefly this orientation representation and use it in Section 3 to derive the simple interdependence between the three orientation angles and the position of the mobile platform of a general 3-*[PP]S* parallel mechanism. Then, in Section 4, we propose closed-form solutions to the direct kinematics of three 3-*[PP]S* parallel mechanisms, namely the 3-$\underline{P}PS$ design proposed in [2] (Fig. 1a), the general 3-$R\underline{P}S$ design (Fig. 1b), and the 3-$\underline{P}RS$ design proposed in [8] (Fig. 1c). Finally, conclusions are given in Section 5.

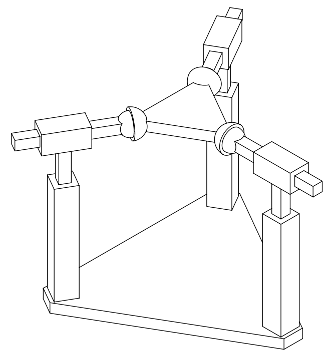

(a) a 3-$\underline{P}PS$ parallel mechanism

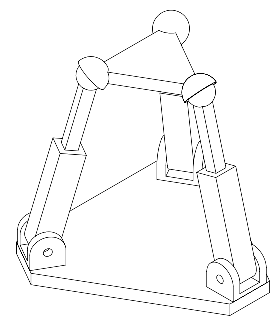

(b) a 3-$R\underline{P}S$ parallel mechanism

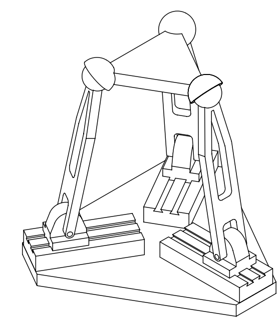

(c) a 3-$\underline{P}RS$ parallel mechanism

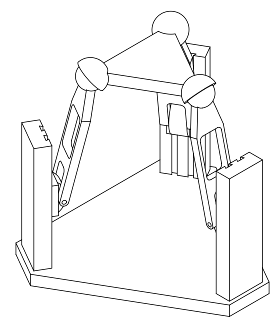

(d) a 3-$\underline{P}RS$ parallel mechanism

Fig. 1. Examples of 3-DOF 3-*[PP]S* parallel mechanisms

[1]It is common to denote parallel mechanisms by using the symbols *P*, *R*, and *S*, which stand respectively for prismatic, revolute, and spherical joint. When a joint is actuated, its symbol is underlined. In this paper, we also use *[PP]* to denote any combination of joints that allows 2-DOF planar motion.

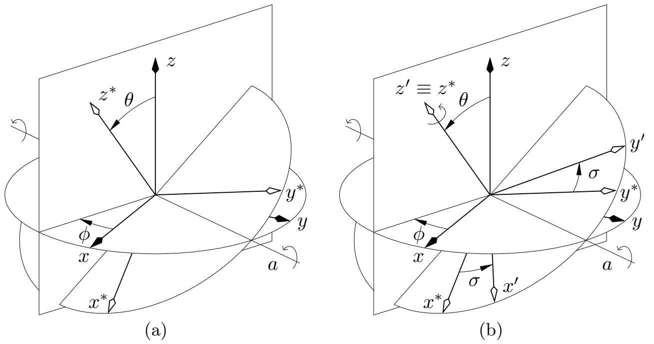

Fig. 2. The successive rotations of the T&T angles: (a) tilt, (b) torsion

II. Orientation Representation

A novel three-angle orientation representation, later called the *Tilt-and-Torsion* (*T&T*) *angles*, was proposed in [14] in 1999, in conjunction with a new method for computing the orientation workspace of symmetric spatial parallel mechanisms. It was shown that the T&T angles take full advantage of a mechanism's symmetry. These angles were also independently introduced in [15] and [16] in 1999. Later, it was found out that the angles had been proposed in [17] in 1984 under the name *halfplane-deviation-twist* angles. The author of that reference proposed the set due to its indisputable advantages in modeling the limits of human body joints. Yet, again in 1999, these angles were proposed independently in [18] as a new standard in modeling angular joint motion, and particularly that of the spinal column's vertebra. These angles are also used for computer animation of articulated bodies, known as the *swing-and-twist* representation. In [12], the advantages of the T&T angles in the study of spatial parallel mechanisms were further demonstrated. It was shown that there is a class of 3-DOF mechanisms that have always a zero torsion, that we now call *zero-torsion parallel mechanisms*. Furthermore, it was demonstrated in [19] and [20] that the workspace and singularities of symmetric spherical parallel mechanisms are best analyzed using the T&T angles.

The T&T angles are defined in two stages—a tilt and a torsion. This does not, however, mean that only two angles define T&T angles but simply that the axis of tilt is variable and is defined by another angle. In the first stage, illustrated in Fig. 2(a), the body frame is tilted about a horizontal axis, a, at an angle θ, referred to as the *tilt*. The direction of axis a is defined by an angle ϕ, called the *azimuth*, which is the angle between the projection of the body z' axis onto the fixed xy plane and the fixed x axis. In the second stage, illustrated in Fig. 2(b), the body frame is rotated about the body z' axis at an angle σ, called the *torsion*.

For space limitations, we will omit the otherwise quite-interesting details of the derivation process (see [12]), and write directly the resulting rotation matrix of the T&T angles, which is

$$\mathbf{R}(\phi,\theta,\sigma) = \begin{bmatrix} c_\phi c_\theta c_{\sigma-\phi} - s_\phi s_{\sigma-\phi} & -c_\phi c_\theta s_{\sigma-\phi} - s_\phi c_{\sigma-\phi} & c_\phi s_\theta \\ s_\phi c_\theta c_{\sigma-\phi} + c_\phi s_{\sigma-\phi} & -s_\phi c_\theta s_{\sigma-\phi} + c_\phi c_{\sigma-\phi} & s_\phi s_\theta \\ -s_\theta c_{\sigma-\phi} & s_\theta s_{\sigma-\phi} & c_\theta \end{bmatrix}, \quad (1)$$

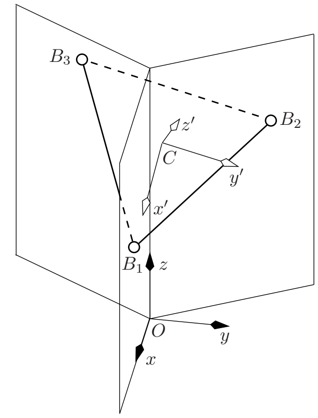

Fig. 3. Kinematic geometry of a general 3-*[PP]S* parallel mechanism

where $c_\phi = \cos\phi$, $s_\phi = \sin\phi$, $c_\theta = \cos\theta$, $s_\theta = \sin\theta$, $c_{\sigma-\phi} = \cos(\sigma-\phi)$ and $s_{\sigma-\phi} = \sin(\sigma-\phi)$.

One of the properties of three-angle orientation representation is that a given orientation can be represented by at least two triplets of angles. In our case, the triplets $\{\phi, \theta, \sigma\}$ and $\{\phi \pm \pi, -\theta, \sigma\}$ are equivalent. To avoid this and the representational singularity at $\theta = \pi$ (which is hardly achieved by any parallel mechanism), we set the ranges of the azimuth, tilt, and torsion as, respectively, $\phi \in (-\pi, \pi]$, $\theta \in [0, \pi)$, and $\sigma \in (-\pi, \pi]$. Then, probably the most valuable property of the T&T angles is that for the ranges just defined, the angles (θ, ϕ, σ) can be represented in a cylindrical coordinate system ($r \equiv \theta$, ϕ, $h \equiv \sigma$) through a one-to-one mapping. In other words, any orientation (except a $\theta = \pi$ one) corresponds to a unique point within a cylinder in the cylindrical coordinate system, and vice versa. The reason is that the T&T representational singularity at $\theta = 0$ is of the same nature as the singularity of the cylindrical coordinate system occurring at zero-radius ($r = 0$).

III. Kinematic Geometry of 3-*[PP]S* Parallel Mechanisms

As already mentioned, each leg of a 3-*[PP]S* parallel mechanisms has a 2-DOF planar chain, followed by an *S* joint. The vertical planes in which the three equidistant *S* joints move are intersecting at a common line at 120° (Fig. 3). Now, let $O-xyz$ be the base reference frame, such that its z axis coincides with the common line of the three planes, and its x axis lies in the plane of leg 1.

For brevity, let the three equidistant *S* joint centers, denoted by B_i, lie on a circle of radius 1, i.e.,

$$\mathbf{r}'_{CB_1} = \begin{bmatrix} 1, 0, 0 \end{bmatrix}^T, \quad (2)$$

$$\mathbf{r}'_{CB_2} = \begin{bmatrix} \cos(2\pi/3), \sin(2\pi/3), 0 \end{bmatrix}^T, \quad (3)$$

$$\mathbf{r}'_{CB_3} = \begin{bmatrix} \cos(4\pi/3), \sin(4\pi/3), 0 \end{bmatrix}^T, \quad (4)$$

where $\mathbf{r}'_{CB_i}$ are the vectors along CB_i expressed in the mobile frame $C-x'y'z'$. We, then, express the coordinates of these three points in terms of the coordinates of the platform center, x, y, z, and the three T&T angles:

$$\mathbf{r}_{OB_i} = \mathbf{R}\mathbf{r}'_{CB_i} + \begin{bmatrix} x \\ y \\ z \end{bmatrix} \equiv \begin{bmatrix} x_{OB_i} \\ y_{OB_i} \\ z_{OB_i} \end{bmatrix}, \tag{5}$$

where $\mathbf{R}$ is the rotation matrix defined by (1) (in this paper, $i = 1, 2, 3$). Then, we write the three linear equations that constrain the *S* joint centers in the three vertical planes:

$$y_{OB_1} = 0, \tag{6}$$

$$\cos(2\pi/3)y_{OB_2} - \sin(2\pi/3)x_{OB_2} = 0, \tag{7}$$

$$\cos(4\pi/3)y_{OB_3} - \sin(4\pi/3)x_{OB_3} = 0. \tag{8}$$

Since z is obviously an independent coordinate, it is of no surprise that, after substitution of y_{OB_1}, x_{OB_2}, y_{OB_2}, x_{OB_3}, and y_{OB_3} from (5), none of the above three equations contains that variable:

$$y + q_{1,3} = 0, \tag{9}$$

$$-\frac{\sqrt{3}}{2}x - \frac{1}{2}y + q_{2,3} = 0, \tag{10}$$

$$\frac{\sqrt{3}}{2}x - \frac{1}{2}y + q_{3,3} = 0, \tag{11}$$

where $q_{1,3}$, $q_{2,3}$, and $q_{3,3}$ are functions of the three T&T angles. Therefore, in order to have a solution for x and y, the three linear equations must be linearly dependent. Obviously, any two of these equations are linearly independent. Hence, for any feasible orientation of the mobile platform, there is a unique solution for $\{x, y\}$.

Let $\mathbf{Q}$ be the coefficient matrix for the above three equations, i.e.,

$$\mathbf{Q} = \begin{bmatrix} 0 & 1 & q_{1,3} \\ -\frac{\sqrt{3}}{2} & -\frac{1}{2} & q_{2,3} \\ \frac{\sqrt{3}}{2} & -\frac{1}{2} & q_{3,3} \end{bmatrix}. \tag{12}$$

For these equations to be linearly dependent, the matrix $\mathbf{Q}$ should be singular, i.e.,

$$\det \mathbf{Q} = \frac{3\sqrt{3}}{4}\sin\sigma(\cos\theta + 1) = 0. \tag{13}$$

Disregarding $\theta = \pi$, (13) leads us to the only remaining possibility: $\sigma = 0$ or $\sigma = \pi$. If we substitute $\sigma = 0$ or $\sigma = \pi$ in (9–11), and solve any two of them, we obtain the following for the feasible motion of the mobile platform center:

$$x = \eth\frac{1}{2}\cos 2\phi(\cos\theta - 1), \tag{14}$$

$$y = -\eth\frac{1}{2}\sin 2\phi(\cos\theta - 1), \tag{15}$$

where $\eth = 1$ for $\sigma = 0$ and $\eth = -1$ for $\sigma = \pi$. These two modes of operation are separated by a *constraint singularity*, which occurs at $\theta = \pi$. Indeed, as shown in [21], constraint singularities generally separate the different modes of operation of constrained parallel mechanisms. While both modes exist in theory, in practice the tilt angle θ will be quite limited, and the actual prototype will be confined to operate in only one of the modes. Furthermore, in practice, the mode $\sigma = \pi$ is hardly realizable. Therefore, for any practical 3-*[PP]S* parallel mechanism, $\sigma = 0$.

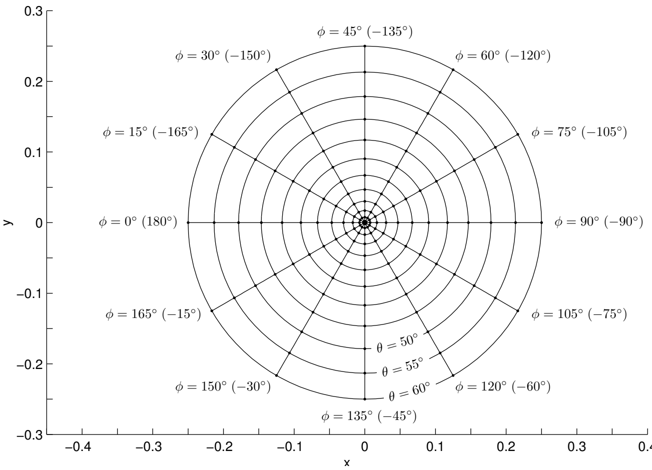

Fig. 4. Horizontal offset as function of orientation for 3-*[PP]S* mechanisms

In industry, zero-torsion parallel mechanisms are used as *plunge-and-tilt* mechanisms with axisymmetric tools. Thus, the lack of knowledge that some torsion angle remains zero does not prevent from successfully operating the mechanism. However, the knowledge of the exact motion of these mechanisms is undoubtedly essential at the design stage and certainly helpful for the development of the control algorithms, since expressions would be more compact. The fact that the center of the mobile platform does not always lie on the central z axis is considered as unwanted motion and should be compensated (through an XY stage). This unwanted motion should, therefore, be well understood.

The mobile platform of a 3-*[PP]S* parallel mechanism has a horizontal offset, υ, from the z axis that is entirely dependent on the tilt of the mobile platform:

$$\upsilon = \frac{1}{2}(1 - \cos\theta). \tag{16}$$

To understand more clearly the coupling between position and orientation, we have shown in Fig. 4 the curves for x and y for constant ϕ or θ (they are obviously independent of z). It should be noted, that for any position of the mobile platform, there are two possible orientations. Their tilts are the same but the azimuths are offset by $180°$. In other words, the platform center moves *away* from the z axis in a direction normal to the tilt plane.

IV. Direct Kinematics of 3-*[PP]S* Parallel Mechanisms

Taking into account that a 3-*[PP]S* parallel mechanism has two separate modes of operation, $\sigma = 0$ and $\sigma = \pi$, is crucial for solving its direct kinematics. Indeed, if we solve the direct kinematics of a 3-*[PP]S* parallel mechanism, without using the T&T angles, we will most probably end with twice the number of solutions. The reason is that half of the solutions are for the mode $\sigma = 0$ and the other half is for the mode $\sigma = \pi$. In other words, the T&T angles simplify greatly the direct kinematics of 3-*[PP]S* parallel mechanisms.

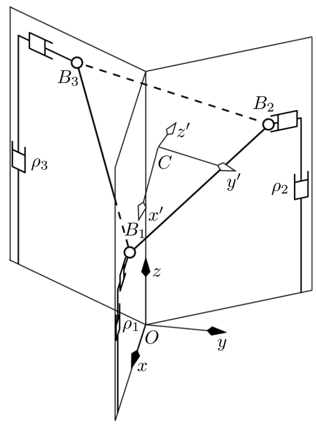

Fig. 5. Schematics of a 3-$\underline{P}PS$ parallel mechanism

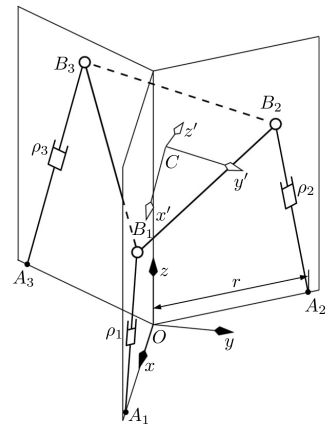

Fig. 6. Schematics of a 3-$R\underline{P}S$ parallel mechanism

A. Direct Kinematics of a 3-$\underline{P}PS$ Parallel Mechanism

Referring to Fig. 5, the directions of the actuated prismatic joints are vertical, while the directions of the passive prismatic joints are horizontal. Let ρ_i be the length of actuator i which is equal to the z coordinate of point B_i. Therefore, we have the following three constraint equations:

$$-c_\phi s_\theta + z - \rho_1 = 0, \tag{17}$$

$$-\frac{\sqrt{3}}{2}s_\phi s_\theta + \frac{1}{2}c_\phi s_\theta + z - \rho_2 = 0, \tag{18}$$

$$\frac{\sqrt{3}}{2}s_\phi s_\theta + \frac{1}{2}c_\phi s_\theta + z - \rho_3 = 0. \tag{19}$$

From the above three equations, we can readily obtain

$$z = \frac{1}{3}(\rho_1 + \rho_2 + \rho_3), \tag{20}$$

$$s_\phi s_\theta = \frac{1}{\sqrt{3}}(\rho_3 - \rho_2), \tag{21}$$

$$c_\phi s_\theta = \frac{1}{3}(\rho_3 + \rho_2 - 2\rho_1). \tag{22}$$

Next, squaring (21) and (22) and adding them, eliminates ϕ, and yields the following solution for s_θ^2:

$$s_\theta^2 = \frac{4}{9}(\rho_1^2 + \rho_2^2 + \rho_3^2 - \rho_1\rho_2 - \rho_2\rho_3 - \rho_1\rho_3). \tag{23}$$

Now, since $0 \leq \theta < \pi$ by definition, its sine is non-negative and we have the following solution:

$$\theta = \sin^{-1}\left(\frac{2}{3}\sqrt{\rho_1^2 + \rho_2^2 + \rho_3^2 - \rho_1\rho_2 - \rho_2\rho_3 - \rho_1\rho_3}\right). \tag{24}$$

This yields two different values in the range $[0, \pi]$, unless $\theta = \pi/2$, which corresponds to a singularity of the mechanism.

Finally, we insert any of the two values for θ into the following equation for ϕ:

$$\phi = \operatorname{atan2}\left(\frac{1}{\sqrt{3}s_\theta}(\rho_3 - \rho_2), \frac{1}{3s_\theta}(\rho_3 + \rho_2 - 2\rho_1)\right). \tag{25}$$

If, however, $\theta = 0$ or $\theta = \pi$, then we do not use the above equation and any ϕ is a solution.

Thus, there are two distinct solutions having the same z and ϕ but different θ. When $\theta = \pi/2$, there is a singularity and the solutions coincide. To conclude this subsection, Table I shows a numerical example with two real solutions.

B. Direct Kinematics of 3-$R\underline{P}S$ Parallel Mechanisms

The direct kinematic problem of this mechanism seems to be the same as that of a hexapod with double spherical joints and planar base. In both cases, the problem is to find the location of an equilateral triangle whose vertices are constrained to move along circles that lie in vertical planes. It was shown in [13], that there are at most 16 real solutions to this problem, which can be obtained by solving a polynomial of degree 8. If, however, we use T&T angles, and set $\sigma = 0$, we should only find eight solutions, in two groups of four (mirror images of the platform). The other eight solutions correspond to $\sigma = \pi$, but we do not need to find them.

Referring to Fig. 6, let the axes of the three revolute joints at the base, being perpendicular to the three constraint planes, lie in the base xy plane and be spaced from the base z axis at a distance r. Let A_i denotes the point at the intersection of the axis of revolute joint i and constraint plane i. Let also ρ_i be the length of leg i. Therefore, we can write the following three constraint equations:

$$(\mathbf{r}_{OB_1} - \mathbf{r}_{OA_1})^T(\mathbf{r}_{OB_1} - \mathbf{r}_{OA_1}) = \rho_1^2, \tag{26}$$

$$(\mathbf{r}_{OB_2} - \mathbf{r}_{OA_3})^T(\mathbf{r}_{OB_2} - \mathbf{r}_{OA_2}) = \rho_2^2, \tag{27}$$

$$(\mathbf{r}_{OB_3} - \mathbf{r}_{OA_2})^T(\mathbf{r}_{OB_3} - \mathbf{r}_{OA_3}) = \rho_3^2, \tag{28}$$

where

$$\mathbf{r}_{OA_1} = \left[\, r, 0, 0 \,\right]^T, \tag{29}$$

$$\mathbf{r}_{OA_2} = \left[\, r\cos(2\pi/3), r\sin(2\pi/3), 0 \,\right]^T, \tag{30}$$

$$\mathbf{r}_{OA_3} = \left[\, r\cos(4\pi/3), r\sin(4\pi/3), 0 \,\right]^T. \tag{31}$$

Next, we substitute $c_\theta = -2\upsilon + 1$ in (26)–(28) (where υ is the offset of the mobile platform center from the z axis),

	ϕ	θ	z
solution 1	171.05°	21.79°	2.03
solution 2	171.05°	158.21°	2.03

TABLE I

AN EXAMPLE OF THE MAXIMUM TWO REAL SOLUTIONS TO THE DIRECT KINEMATICS OF A 3-$\underline{P}PS$ PARALLEL MECHANISM FOR WHICH $\rho_1 = 2.40$, $\rho_2 = 1.80$, $\rho_3 = 1.90$ AND $\sigma = 0$

replace (27) with the difference between (27) and (28), and (28) with the sum of (27) and (28), and obtain the following three equations after rearranging:

$$z^2 + p_{1,2}\, z + p_{1,3} \;=\; 0, \tag{32}$$
$$p_{2,2}\, z + p_{2,3} \;=\; 0, \tag{33}$$
$$2z^2 + p_{3,2}\, z + p_{3,3} \;=\; 0, \tag{34}$$

where

$$\begin{aligned}
p_{1,2} &= -2s_\theta c_\phi,\\
p_{1,3} &= 4vc_\phi^2(4vc_\phi^2 - 3v + 2r - 1) + (1 + v - r)^2 - \rho_1^2,\\
p_{2,2} &= -2\sqrt{3}s_\theta s_\phi,\\
p_{2,3} &= 4\sqrt{3}vs_\phi c_\phi(4vc_\phi^2 - 3v - 2r + 1) - \rho_2^2 + \rho_3^2,\\
p_{3,2} &= 2s_\theta c_\phi,\\
p_{3,3} &= -4vc_\phi^2(4vc_\phi^2 - 3v + 2r - 1)\\
&\quad +2(1 - 2r - v + v^2 + 4rv + r^2) - \rho_2^2 - \rho_3^2.
\end{aligned}$$

Therefore, in order to have a solution for z, the three equations must be linearly dependent. Let $\mathbf{P}$ be the coefficient matrix for the above three equations, i.e.,

$$\mathbf{P} = \begin{bmatrix} 1 & p_{1,2} & p_{1,3} \\ 0 & p_{2,2} & p_{2,3} \\ 2 & p_{3,2} & p_{3,3} \end{bmatrix}. \tag{35}$$

For these equations to be linearly dependent, matrix $\mathbf{P}$ should be singular, i.e.,

$$\det \mathbf{P} = 2\sqrt{3}s_\theta\big(6\sin(3\phi)(2r - 1)v - d\big) = 0, \tag{36}$$

where

$$d = 2s_\phi\rho_1^2 - (s_\phi + \sqrt{3}c_\phi)\rho_2^2 - (s_\phi - \sqrt{3}c_\phi)\rho_3^2. \tag{37}$$

It can be easily verified that $\theta = 0$ is a solution to (26)–(28), if and only if all three leg lengths are equal. Therefore, since $\theta = \pi$ is not a feasible solution in practice, we can disregard the case $s_\theta = 0$, assuming that the leg lengths are not all equal. Thus, we obtain the following relationship for the offset v (i.e., for $\cos\theta$):

$$v = \frac{d}{6\sin(3\phi)(2r - 1)}. \tag{38}$$

Since in practice, the base is always larger than the mobile platform (i.e, $r > 1$), we do not need to worry about zeroing the denominator of v with $r = 0.5$. However, we should study the case $\sin(3\phi) = 0$. It can be verified that when $\sin(3\phi) = 0$, the determinant of $\mathbf{S}$ is zeroed uniquely if two of the leg lengths are equal (or if $s_\theta = 0$). Therefore, the case when two leg lengths are equal should be studied separately.

Now, adding (32) and (34), and rearranging yields:

$$z^2 = \frac{1}{3}(\rho_1^2 + \rho_2^2 + \rho_3^2) - 1 + 2r - r^2 - 2rv - v^2. \tag{39}$$

In other words, we have a simple expression for z^2 as a function of v only, which is a function of ϕ only. However, we can also find an expression for z from (33):

$$z = -\frac{p_{2,3}}{p_{2,2}}, \tag{40}$$

provided that neither $\sin\phi = 0$ nor $\sin\theta = 0$. As already discussed, these can only be zero when two or all three of the leg lengths are equal.

Finally, we square the right-hand side of (40) and set it equal to the right-hand side of (39), substitute $c_\theta = -2v+1$ where v is replaced with the right-hand side of (38), and then apply double-angle formulas for ϕ. After rearranging, simplifying and taking only the numerator, we have the following equation (which runs about a page when the coefficients are expanded):

$$\begin{aligned} w_1\cos(2\phi)^2 + w_2\cos(2\phi)\sin(2\phi) + w_3\cos(2\phi)&\\ +w_4\sin(2\phi) + w_5 = 0,& \end{aligned} \tag{41}$$

where $w_1, w_2, ..., w_5$ are coefficients depending on ρ_1, ρ_2, ρ_3, and r only and will not be presented here.

The above equation can be easily solved by performing the tangent-half-angle substitution:

$$\sin(2\phi) = \frac{2t}{1+t^2},\ \cos(2\phi) = \frac{1-t^2}{1+t^2}, \tag{42}$$

where $t = \tan\phi$. After substituting the above identities in (41), multiplying by $(1+t^2)^2$, and rearranging, we obtain

$$u_4t^4 + u_3t^3 + u_2t^2 + u_1t + u_0 = 0, \tag{43}$$

where $u_4 = w_1 - w_3 + w_5$, $u_3 = 2(w_4 - w_2)$, $u_2 = 2(w_5 - w_1)$, $u_1 = 2(w_2 + w_4)$ and $u_0 = w_1 + w_3 + w_5$.

The solutions for t may be found analytically by solving the polynomial of degree four in (43). Then, for each real solution for t, we obtain the corresponding value for ϕ using $\phi = \tan^{-1} t$. Note, however, that $\tan\phi$ is not defined at $\phi = \pi/2$. Therefore, this potential solution should be tested manually in (41).

Thus, from (43), we obtain eight different solutions for ϕ, since from each t, we have two different values for ϕ, whose difference is π. Then, we substitute each value of ϕ in (38) and find a corresponding positive value for θ (recall that we have defined θ to be positive). Note that θ is the same for both ϕ and $\phi+\pi$, so we have at most four distinct tilt angles. Finally, we substitute each ϕ and θ into (40) to find the corresponding z. Note that the value of z differs only in sign for ϕ and $\phi+\pi$.

Before concluding this section, we should study the case when two or three of the leg lengths are equal. Note that if all three leg lengths are equal, then (43) becomes $0 = 0$ and we need to follow another similar yet simpler procedure to find the solutions, one of which has $\theta = 0$. When only two legs are of equal length, (43) is valid and can still be used. However, four of the maximum eight real solutions for ϕ are such that $\sin(3\phi) = 0$. Therefore, they cannot be substituted in (38) to find θ and then z. Similarly, another procedure should be followed in order to obtain the corresponding solutions. We will, however, skip the presentation of these procedures for the sake of brevity.

To conclude this subsection, Table II shows a numerical example with all eight possible real solutions.

	ϕ	θ	z
solution 1	$14.53°$	$91.58°$	2.29
solution 2	$194.53°$	$91.58°$	-2.29
solution 3	$53.75°$	$107.03°$	-2.11
solution 4	$233.75°$	$107.03°$	2.11
solution 5	$-71.82°$	$56.02°$	-2.64
solution 6	$108.18°$	$56.02°$	2.64
solution 7	$-78.46°$	$37.94°$	-2.75
solution 8	$101.54°$	$37.94°$	2.75

TABLE II

AN EXAMPLE OF THE MAXIMUM EIGHT REAL SOLUTIONS TO THE DIRECT KINEMATICS OF A 3-*RPS* PARALLEL MECHANISM FOR WHICH $r = 2.50$, $\rho_1 = 3.20$, $\rho_2 = 2.80$, $\rho_3 = 3.60$ AND $\sigma = 0$

C. Direct Kinematics of a 3-PRS Parallel Mechanism

Finally, let us consider a more complex architecture of the 3-*[PP]S* family, namely the 3-*PRS*. The direct kinematics of the general 3-*PRS* is somewhat more intricate and implies the solution of a univariate polynomial of degree 8. However, the direct kinematic problem of a 3-*PRS* parallel mechanism for which the axes of the revolute joints remain in the xy plane (Fig. 1c) can be solved using exactly the same procedure as the one outlined in the previous subsection. Since, the expressions are, however, quite larger, we will not present them here.

V. CONCLUSIONS

We presented in this paper yet another example of the advantages of using Tilt-and-Torsion angles for the analysis of 3-DOF zero-torsion parallel mechanisms. In particular, we proposed, for the first time, solutions to the direct kinematics of three different zero-torsion mechanisms, namely a 3-*PPS* design, the general 3-*RPS* design, and a 3-*PRS* design. Furthermore, these solutions are in closed-form and correspond only to one of the two possible operational modes. It should now be clear that so-called zero-torsion parallel mechanisms must be analyzed using Tilt-and-Torsion angles only.

REFERENCES

[1] Merlet, J.-P., *Parallel Robots*, 2nd ed., Springer, the Netherlands, 2006.

[2] Liu, X.-J., Pruschek, P., and Pritschow, G., "A new 3-DoF parallel mechanism with full symmetrical structure and parasitic motions," *Proceedings of the Intelligent Manipulation and Grasping International Conference*, Genova, Italy, pp. 389–394, 2004.

[3] Lee, K.-M., and Shah, D.K., "Kinematic analysis of a three-degree-of-freedom in-parallel actuated manipulator," *IEEE Journal of Robotics and Automation*, Vol. 4, No. 3, pp. 354–360, 1988.

[4] Buruncuk, K., and Tokad, Y., "On the kinematics of a 3-DOF Stewart platform," *Journal of Robotic Systems*, Vol. 16, No. 2, pp. 105–118, 1999.

[5] Kim, H.S., and Tsai, L.-W., "Kinematic synthesis of a spatial 3-RPS parallel manipulator," *ASME Journal of Mechanical Design*, Vol. 125, pp. 92–97, 2003.

[6] Liu, C.H., and Cheng, S., "Direct singular positions of 3RPS parallel manipulators," *ASME Journal of Mechanical Design*, Vol. 126, pp. 1006–1016, 2004

[7] Sokolov, A., and Xirouchakis, P., "Singularity analysis of a 3-DOF parallel manipulator with R-P-S joint structure," *Robotica*, Vol. 24, No. 1, pp. 131–142, 2006.

[8] Carretero, J.A., Nahon, M.A., and Podhorodeski, R.P., "Workspace analysis and optimization of a novel 3-DOF parallel manipulator," *IEEE Journal of Robotics and Automation*, Vol. 15, No. 4, pp. 178–188, 2000.

[9] Tsai, M.-S., Shiau, T.-N., Tsai, Y.-J., and Chang, T.-H., "Direct kinematic analysis of a 3-PRS parallel mechanism," *Mechanism and Machine Theory*, Vol. 38, No. 1, pp. 71–83, 2003.

[10] Wahl, J., "Articulated tool head," WIPO Patent No. WO 00/25976, 2000.

[11] Li, J., Wang, J., Chou, W., Zhang, Y., Wang, and Zhang, Q., "Inverse kinematics and dynamics of the 3-RRS parallel platform," *Proceedings of the IEEE International Conference on Robotics and Automation*, Seoul, Korea, pp. 2506–2511, 2001.

[12] Bonev, I.A., Zlatanov, D., and Gosselin, C.M., "Advantages of the modified Euler angles in the design and control of PKMs," *Parallel Kinematic Machines International Conference*, Chemnitz, Germany, pp. 171–188, 2002.

[13] Nanua, P, Waldron, K.J., and Murthy, V., "Direct kinematic solution of a Stewart platform," *IEEE Transactions on Robotics and Automation*, Vol. 6, No. 4, pp. 438–443, 1990.

[14] Bonev, I.A., and Ryu, J., "Orientation workspace analysis of 6-DOF parallel manipulators," *Proceedings of the ASME 1999 Design Engineering Technical Conferences*, Las Vegas, NV, 1999.

[15] Huang, T., Wang, J., and Whitehouse, D.J., "Closed form solution to workspace of hexapod-based virtual axis machine tools," *Journal of Mechanical Design*, Vol. 121, pp. 26–31, March 1999.

[16] Wang, Y., "Workspace analysis of a novel closed-chain manipulator," *Thesis*, Case Western Reserve Univ., Cleveland, OH, 1999.

[17] Korein, J.U., *A Geometric Investigation of Reach*, MIT Press, 1984.

[18] Crawford, N.R., Yamaguchi, G.T., and Dickman, C.A., "A new technique for determining 3-D joint angles: The tilt/twist method," *Clinical Biomechanics*, Vol. 14, No. 3, pp. 153–165, 1999.

[19] Bonev, I.A., and Gosselin, C.M., "Singularity loci of spherical parallel mechanisms," *Proceedings of the IEEE International Conference on Robotics and Automation*, Barcelona, Spain, pp. 2968–2973, 2005.

[20] Bonev, I.A., and Gosselin, C.M., "Analytical determination of the workspace of symmetrical spherical parallel mechanisms," *IEEE Transactions on Robotics*, Vol. 22, No. 5, pp. 1011–1017, 2006.

[21] Zlatanov, D., Bonev, I.A., and Gosselin, C.M., "Constraint singularities of parallel mechanisms," *Proceedings of the IEEE International Conference on Robotics and Automation*, Washington, DC, USA, pp. 496–502, 2002.